Egyptian Journal of Anatomy, Jul. 2017; 40(2):358-380

Original Article

The effect of immobilization induced stress on the lung of the adult male albino rat and the possible protective role of melatonin: A light, electron microscopic and immunohistochemical study

Heba K. Mohamed

Human Anatomy and Embryology Department, Faculty of Medicine, Assiut University, Egypt

ABSTRACT

Background: Stress is known as one of the most important reasons of many diseases. Immobilization is one of the most common performed stresses on animals. immobilization stress may induce the formation of reactive oxygen species and can lead to suppression of immune system. Melatonin as an antioxidant, has an important role in the immune function. The lung has a large surface that is constantly in contact with air oxygen and pollutants. It is one of the organs commonly affected by reactive oxygen species generation which induces oxidative damage. It is a site of major reactive oxygen species production.

Aim of work: The present study aimed to investigate the effect of immobilization induced stress on the lung in the adult male albino rat and the possible protective role of melatonin.

Material and Methods: 45 adult male albino rats weighing 200–250 g were used in this study. The rats were randomly divided into three equal groups (15 rats each). Group (I): the rats kept undisturbed and served as non-stress control group. They were sacrificed at the end of the experiment. Group (II): the rats subjected to stress and placed on a wooden plate with their trunks wrapped in a confining harness for 90 min 5 days/ week for 6 weeks. The animal was able to move its limbs and head but not its trunk. Group (III): the rats were exposed to stress as previously described and concurrently injected melatonin intraperitoneally in a dose of 10 mg/kg/day at 4:00 pm. All animals were sacrificed by decapitation under anaesthesia at the same time, then lungs dissected out. The specimens of each group were randomly divided into three subgroups; the first was processed for the light microscopic study (H & E), the second for the transmission electron microscopic study and the third for the immunohistochemical study (Caspase-3 and iNOS). Morphometric studies and statistical analysis were performed.

Results: The light microscopic and ultrastructural examination of the rat lungs after immobilization showed severe alveolar damage in the form of collapsed alveolar saccule and alveoli, markedly thickened interalveolar septa encroaching on alveoli, heavy inflammatory cellular infiltration and exudation. Pneumocyte type I showed indentation of its nuclear membrane, presence of chromatin clumps inside the nucleus and swollen mitochondria with disrupted cristae. Melatonin treated group revealed an evident reduction of all alveolar changes with nearly normal structure of the alveolar ducts, alveolar saccules and alveoli. Immunohistochemically stained lung sections for caspase-3 and iNOS after immobilization showed an intense brownish immune reactions. Melatonin treated group revealed a noticeable reduction in the immune reactions.

Conclusion: Immobilization stress has a damaging effect on the histological structure of the lung and a concomitant treatment with an antioxidant (melatonin) effectively protected the lung tissue.

Key Words: Immobilization stress, lung, melatonin.

Corresponding Author: Heba K. Mohamed, Human Anatomy and Embryology Department, Faculty of Medicine, Assiut University, Assiut, Egypt, **Email:** hebaelgamae73@yahoo, **Mobile:** 01001016547

INTRODUCTION

The psychological factors have long been suspected to influence the lung function in asthma. The impact of various emotional states and stressful challenge on the airways was investigated in health and asthma *(Ritz and Kullowatz, 2005)*. Stress remains a clinically relevant factor for asthmatics. In addition, several epidemiological studies showed that 20–35% of asthmatics experiencing exacerbations occur during the periods of stress (*Ritz et al., 2000; Liu et al., 2002; Hoglund et al., 2006*). A tendency of bronchoconstriction in asthmatics under negative emotional conditions was also reported (*Ritz et al., 2000*).

 DOI: 10.21608/EJANA.2018.16911

Stress can be defined as physical and psychological modifications that disrupt the homeostasis and the balance of organisms. Stress is known as one of the most important reasons of many diseases (*Johnson et al., 1992*). It has been reported that there are some forms of stress, such as exercise, trauma, major surgery, starvation, radiation, emotional and oxidation stress etc., in addition, initiation of lipid peroxidation due to increase in the free radical generation (*Demling et al. 1986; Wohaieb and Godin 1987; Hidalgo et al. 1988*). Different stress types have been associated with enhanced free radical generation and altered antioxidant enzyme activities (*Giralt et al., 1993; Liu et al., 1994; Bian et al., 1997; Seckin et al., 1997; Gumuslu et al., 2002*). Moreover, it has been proposed that free radical processes might be involved in the control of general physiological response to stress (*Kovacheva-Ivanova et al., 1994*). Many different types of stress induce changes in the immune system, so, there is a relation between stress and developing certain kinds of cancer as well as increased serum level of tumor markers (*Wright et al., 1998*). Stresses result in immune system suppression in laboratory animals (*Dhabhar and McEwen, 1999*). The stress response can activate the adrenomedullary system and hypothalamic-pituitary-adrenal axis, leading to a release of glucocorticoids and catecholamines which, in turn, could influence the immune system and the course of diseases (*Wright et al., 1998; Ritz et al., 2000; Wright et al., 2005*).

Immobilization is one of the most common performed stresses on animals (*Jaggi et al., 2011*). It takes up an important position among different forms of stress (*Meerson, 1984*). Acute or chronic immobilization considered as one of the various stress types that has been used extensively and accepted widely for studying the association between stress and pathophysiological alterations (*Marić et al., 1996*). The immobilization stress can lead to suppression of the immune system. Repeated immobilization stress causes structural changes in areas of the brain responsible for emotional memories and regulation of the stress response (*Li et al., 1997; Miller and McEwen, 2006*). However, there are studies showing that acute stress enhances immune function but chronic stress suppresses the immune system (*Dragoş and Tănăsescu, 2010*).

Melatonin (N-acetyl-5-methoxytryptamine) is the main secretory product of the pineal gland in all mammals including humans, but it is also produced in other organs (*Okutan et al., 2004*). It has been shown that melatonin has an important role in the immune function under both physiological and physiopathological conditions (*Maetroni, 2001*). An increase in the capacity of macrophages to phagocytize antigens during the dark period in mice was observed when melatonin concentration is elevated (*Barriga et al., 2001*). Melatonin is an important regulator of the circadian rhythm and has antioxidizing and anti-inflammatory properties (*Reiter et al., 2007; Carloni et al., 2008*). It was reported that melatonin reduces the oxidative stress (*Gitto et al., 2009*) and lipid peroxidation products (*Fulia et al., 2001*), suggesting that melatonin may be an effective protective agent (*Gitto et al., 2011*).

AIM OF WORK

So, this study aimed to investigate the effect of i mmobilization induced stress on the lung in the adult male albino rat and the possible protective role of melatonin by a light, electron microscopic and immunohistochemical study.

MATERIAL AND METHODS

Animals

45 adult male albino rats weighing on average 200–250 g were used in this study. The rats were obtained from the Animal House, Faculty of medicine, Assiut University, Egypt. They were kept under suitable conditions for 1 week for adaptation. They were maintained in stainless steel cages in a well-ventilated animal house at normal temperature (22°C ± 5°C) under a 12:12-hour light–dark cycle. They were fed with standard diet and given water ad libitum throughout the study in accordance with the international guidelines for the care and use of laboratory animals.

Chemicals:

- Melatonin (Sigma–Aldrich, St. Louis, Mo., USA).

- Caspase-3 was purchased from Thermo scientific Company, USA. (Runcorn, Cheshire

WA71CA, UK.). Other reagents were of analytical grade and were obtained from commercial sources.

 Inducible nitric oxide synthase (iNOS) was purchased from Thermo Scientific Company, USA.

Experimental protocol

The rats were randomly divided into three equal groups (15 rats each).

- **Group I (Control group)**: The rats will be kept undisturbed and served as non-stress control group. They will be sacrificed at the end of the experiment.

- **Group II (Stressed group)**: rats will be subjected to stress. They will be placed on a wooden plate with their trunks wrapped in a confining harness for 90 min 5 days/week for 6 weeks. The animal was able to move its limbs and head but not its trunk (*Bertsch et al., 2013*).

- **Group III (Melatonin-treated stressed group)**: rats will be exposed to stress as previously described and concurrently injected melatonin (Sigma–Aldrich, St. Louis, Mo., USA). Melatonin was dissolved a vehicle composed of 1% ethanol and 99% distilled water (*Abd-Allah et al., 2003*) and injected intraperitoneally (i.p.) in a dose of 10 mg/kg/day at 4:00 pm (*Bassani et al., 2014*).

At the end of the experiment, all animals were sacrificed by decapitation under anaesthesia at the same time, then the lungs dis-sected out and processed for light, electron microscopic and immunohistochemical study. The specimens of each group (control, stressed and melatonin-treated stressed rats) were randomly divided into three subgroups; the first was processed for the light microscopic study, the second for the electron microscopic study and the third for the immunohistochemical study.

Light microscopic study

The tissues were immediately fixed in neutral buffered 10% formalin solution, and processed into 5um-thick paraffin sections, then stained with hematoxylin & eosin (H&E) (*Bancroft and Gamble, 2007*). The stained sections of the lung were examined under the light microscope.

Electron microscopic study

Ultrastructural study of the lung in all groups was done. The specimens were fixed in fresh 3% glutaraldehyde at 4 Ċ for 4 h. Then, 1mm specimens were cut and washed in 0.15mol/l phosphate buffer, pH 7.4, for 2h (two changes), then postfixed in 1% osmium tetroxide for 1 h at 4°Ċ. The specimens were dehydrated and embedded in epoxy resin. Semithin sections were cut at (0.5–1um) thickness by an ultramicrotome and stained with 1% toluidine blue. Ultrathin sections (50–80 nm thick) from selected areas were cut using the same ultramicrotome and stained with uranyl acetate and lead citrate (*Hayat, 2000*). The sections were examined using the transmission electron microscope 'Jeol-JEM-100 CXII' at the electron microscopic unit, (Akishima, Tokyo, Japan), Assiut University.

Immunohistochemical study

Caspase-3 (Rabbit Polyclonal Antibody) was used for the detection of apoptosis in the lung cells. Paraffin sections of the lungs of different groups and of a positive control (tonsils) were cut into 5 µm thickness on positively charged slides and incubated at 42°C in an oven for 24 h. The sections were deparaffinized in xylene (1 h), hydrated in descending grades of alcohol, and then incubated in hydrogen peroxide (5 min). They were then washed twice in PBS (5 min each). The primary antibody (diluted 1:100) was applied to the sections, which were then incubated for 1.5 h. Thereafter, the sections were washed twice in PBS for 5 min each. The secondary antibody was applied and the sections were again incubated for 20 min, following which they were washed three times in PBS for 5 min each. Diaminobenzidine tetra hydrochloride solution was then applied to the sections and they were further incubated for 10 min (Bancroft and Gamble, 2002). The sections were then washed in distilled water and counterstained with Mayer's hematoxylin (2 min), following which they were washed in tap water, dehydrated, cleared, and mounted by DPX. Negative controls were processed according to the same protocol, except for the use of the primary antibody.

Paraffin sections were immunohistochemically stained for detection of inducible nitric oxide synthase (iNOS). A streptavidin system with antibody against the iNOS marker for

oxidative stress was used to carry out the immunohistochemical reaction. The sections were deparaffinized, hydrated, washed in 0.1 mol/l PBS, treated with trypsin 0.01% for 10 min at 37°C, and then washed with PBS for 5 min. Blockage of endogenous peroxidases was done by treatment with 0.5% H2O2 in methanol. Nonspecific binding was blocked in normal goat serum diluted 1:50 in 0.1 mol/l PBS. Sections were incubated with the primary antibody (Polyclonal Rabbit Anti-iNOS); which was diluted 1:100 overnight at 4°C. The universal kit used was biotinylated secondary antibodies. The immune reaction was detected with 0.05% diaminobenzidine and the slides were counter stained with Mayer's hematoxylin before mounting. Brown coloration of the cytoplasm indicated positive results for the iNOS immune reaction (Kiernan, 2001). For negative controls, normal rat serum (×100 diluted) were used instead of the primary antibody.

Morphometric procedure and Statistical Study

The immunohistochemically stained sections for detection of iNOS were analyzed morphometrically using an image analyzer computer system. The data were obtained using a computer-based image analysis software (soft imaging system-An OPTIMAS version 6.2.1 program - Adept turnkey, Sydney, Australia). This image analyzer computer system was used to evaluate the optical density (OD) of the iNOS immune reaction. The OD of the iNOS immune reaction was measured in the cytoplasm of the lining epithelial cells of alveolus, bronchioles, bronchiolar arterioles, interalveolar wall, the cells of connective tissue between bronchiolar arterioles, the cells of thickened interalveolar wall and among an area of inflammatory cells infiltration using the gray measure menu in 10 measuring frames in each specimen using an objective lens of magnification X40.

All data were expressed as mean ± standard deviation (SD). Histograms were constructed and statistical analysis was done through a student's (t) test to compare the means between the different groups. The P value was calculated using (GraphPad Software program - San Diego, California, USA) and level of significance (p) value was considered as follows: (i) $p > 0.05$, non-significant; (ii) $p \leq 0.05$, significant.

RESULTS

I. Light microscopic results

A- Hematoxylin and eosin stain

Examination of lung sections of the control rats revealed normal lung architecture including the alveoli, alveolar ducts and alveolar saccules. The alveolar saccule is a large alveolar sac fomed by fusion of alveoli together. The alveoli appeared patent with a thin alveolar wall and thin interalveolar septa. The septae were formed of thin and thick portions and consisted of an alveolar epithelium, capillaries, and a delicate connective tissue. Relatively few, thin and short poorly developed secondary septae were observed. The lining epithelium of the alveoli was composed of squamous cells with flattened nuclei (flat pneumocyte type I) and large cuboidal cells with large rounded nuclei (pneumocyte type II). A normal branch of the pulmonary artery and a bronchiole which is lined by respiratory epithelium (pseudostratified columnar ciliated epithelium) and surrounded by bundles of spirally arranged smooth muscle fibers were observed (Figs 1 and 2).

Sections of the lung of group II showed severe alveolar damage in the form of collapsed alveolar saccule and alveoli, markedly thickened interalveolar septa encroaching on alveoli, heavy inflammatory cellular infiltration and exudation. Dilated congested branch of pulmonary artery and blood capillaries with extravasation of red blood cells (RBCs) within the alveolar lumen were also detected. Respiratory bronchioles lined by ciliated columnar epithelium and a non-ciliated Clara cell were observed with surrounding lamina propria under the bronchiolar epithelium, thickened layer of smooth muscle and connective tissue. Moreover, most of them showed exfoliation of many cells from their lining epithelium and cellular debris in their lumina associated with RBCs (Figs 3, 4, 5 and 6).

Examination of lung sections of group III revealed evident reduction of all alveolar changes. Nearly normal structure of alveolar ducts, alveolar saccules and alveoli which are lined by simple squamous epithelium (flat pneumocytes type I) and pneumocytes type II

was detected. The interalveolar septa was thin except in a few areas. The bronchioles appeared lined by respiratory epithelium and surrounded by smooth muscles which appeared relatively thin in comparison with those in group II (Figs 7 and 8).

B- Toluidine blue stain

Sections of the control rats showed normal structure of the alveolar saccule and alveolus which is lined by flat pneumocyte type I and few rounded pneumocyte type II with vacuolated cytoplasm. The primary interalveolar septa is formed of variable-size interstitial cells with pale irregular nuclei and vacuolated cytoplasm, whereas other cells revealed dark flat nuclei. Relatively short thin secondary septae with elongated cells were observed. Blood capillaries were noticed (Figs 9 and 10).

Examination of lung sections in group II revealed collapsed alveoli which had pneumocyte type II with large irregular nuclei and maked cytoplasmic vacuolations. Degenerated cells can be noticed. The thickened interalveolar septa revealed many vacuolated areas, areas of degenerations, cells with irregular nuclei and vacuolated cytoplasm and other cells with fragmented nuclei. Note separation of the epithelium from its underlying basement membranes in some bronchioles (Figs 11, 12 and 13).

In group III, lung sections revealed nearly normal alveoli lined by flat pneumocytes type I and pneumocytes type II which are nealy normal. The interalveolar septa appeared thin except in a few areas.The bronchial walls relatively maintained their continuity with the underlying basement membrane (Fig 14).

II. Immunohistochemical results

1- Immunohistochemical stain for caspase-3

Immunostained sections of the lung in the control group revealed a negative cytoplasmic immune reaction for caspase-3 along the lining epithelial cells of alveolar wall and interalveolar septa (Fig 15).

Lung sections in group II showed an intense brownish cytoplasmic immune reaction in the lining epithelial cells of bronchiole, alveoli, interalveolar septa, endothelial lining of some blood vessels and along the exfoliated bronchial epithelial cells (Figs 16 and 17).

In group III, the sections revealed a slight cytoplasmic immune reaction along the alveolar epithelial lining as compared with group II (Fig 18).

2- Immunohistochemical stain for iNOS

Lung sections of the control group showed a weak immune reaction to iNOS in the lining epithelial cells of alveolar wall and along the interalveolar septa (Fig 19).

In group II, there was an intense iNOS expression as a brown cytoplasmic immune reaction along the alveolar epithelium, lining epithelial cells of the bronchiole and along the endothelial lining of some blood vessels. A strong iNOS expression was also noticed in the cells of thickened interalveolar septa and among an area of inflammatory cellular infiltration (Figs 20 and 21).

The sections of group III showed moderate iNOS expression in the lining epithelial cells of alveoli and interalveolar septa (Fig 22).

III. Electron microscopic results

Ultrathin lung sections of the control group revealed two types of pneumocytes that form the alveolar cell lining. The flattened pneumocyte type I, which is the predominant cell type each with a single flat nucleus surrounded by a narrow perinuclear cytoplasm containing mitochondria and rough endoplasmic reticulum (Fig 23). Type II pneumocytes appeared cuboidal in shape, with a large euchromatic nucleus and a few short microvilli on their cell surface. The most characteristic feature of these cells is the presence of lamellar bodies in their cytoplasm. Mitochondria with variable sizes and shapes can be noticed. The interstitial connective tissue had a fibroblast (Figs 23 and 24). Alveolar macrophages were encountered in the interstitial connective tissue which appeared with large, indented nuclei, many lysosomes, mitochondria and rough endoplasmic reticulum (Fig 25).

In group II, lung sections showed pneumocyte type I with indentation of its nuclear membrane and presence of chromatin clumps inside the nucleus. Swollen mitochondria with disrupted cristae and cytoplasmic vacuolations were noticed (Fig 26). Pneumocyte type II revealed swollen mitochondria with disrupted cristae and vacuolated lamellar bodies which were relatively deprived of their content of secretory surfactant material leaving irregular empty spaces associated with collagen fiber deposition. Many cells showed an apparent increase in the size of their lamellar bodies when compared with the control group and most of them appeared vacuolated (Figs 26, 27 and 28). Some cells appeared electron dense with electron dense nucleus, phagosomes and swollen electron dense mitochondria. Other cells showed fragmented nucleus. Numerous collagen fibers deposited in the interstitium were observed (Figs 28 and 29). Many large macrophages with large indented nuclei were present in the alveolar spaces and in the lung interstitium. Their cytoplasm had swollen mitochondria with disrupted cristae and dilated rough endoplasmic reticulum, lysosomes. Dilated perinuclear cisternae can be seen (Fig 30).

Lung sections of group III showed considerable degree of preservation of alveolar architecture. Pneumocyte type – I had a flat nucleus and surrounding narrow perinuclear cytoplasm which revealed apparently healthy mitochondria and rough endoplasmic reticulum (Fig 31). Type II pneumocytes still showed some vacuolated lamellar bodies which were relatively deprived of their secretion. The cytoplasm contained rough endoplasmic reticulum and mitochondria which appeared healthy with variable sizes. Short microvilli on the cell surface can be detected (Fig 32). Alveolar macrophages had a large indented nucleus and pseudopodia. Their cytoplasm contained Mitochondria, lysosomes and dilated rough endoplasmic reticulum (Fig 33).

IV. Morphometrical and Statistical Results

There was a significant increase in the means of the optical density of iNOS in group II, in comparison to group I. Also, there was a significant decrease in the means of optical density of iNOS in group III in comparison with group II (Table 1 and Histogram 1).

Table 1: The mean values ± SD of the optical density of iNOS of the different groups.

Groups	Mean ± SD
Control group (GI)	0.18 ± 0.040
Stress group (GII)	0.35 ± 0.058
Stress+melatonin treated (GIII)	0.24 ± 0.044
P (I vs. II)	0.0001*
P (II vs. III)	0.0001*

* Extremely statistically significant difference.

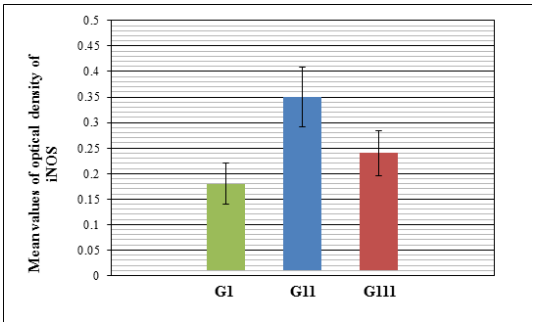

Histogram 1: Mean values of the optical density of iNOS of the control group (GI), stress group (GII) and stress + melatonin treated group (GIII). Error bars represent standard deviation.

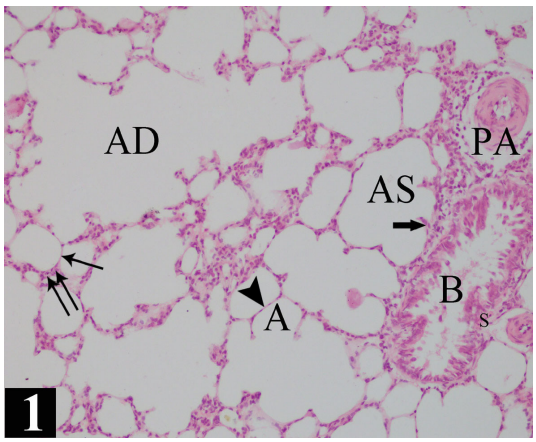

Fig. 1: A photomicrograph of a section in the lung of a control rat showing normal structure of the alveolar duct (AD), alveolar saccule (AS) and alveolus (A) which is lined by simple squamous epithelium (arrow head) and has a wide lumen. Note the primary interalveolar septa which is formed of a thin (thin arrow) and a thick (double arrow) portions. Short thin secondary septa (thick arrow) appear bulging into the saccular lumen. A branch of pulmonary artery (PA) and a respiratory bronchiole (B) which is surruounded by smooth muscles (S) are seen. H & E, X200.

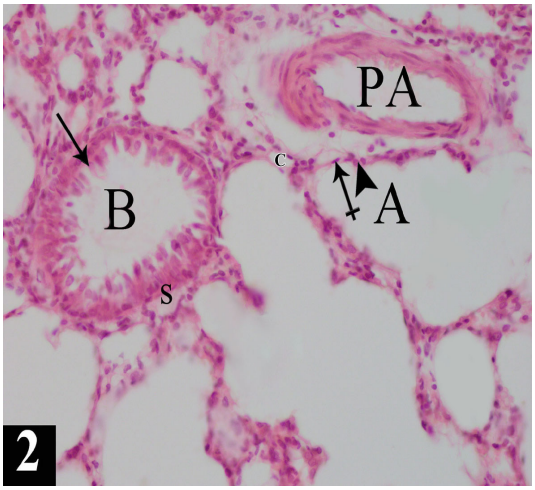

Fig. 2: A photomicrograph of a section in the lung of a control rat showing a normal structure of an alveolus (A) which is lined by a flat pneumocyte type I (crossed arrow) and a pneumocyte type II (arrow head). A bronchiole (B) lined by respiratory epithelium (arrow) and surruounded by smooth muscles (S) is observed. Note a branch of pulmonary artery (PA). A blood capillary (C) can be seen in the interalveolar septa. H & E, X400.

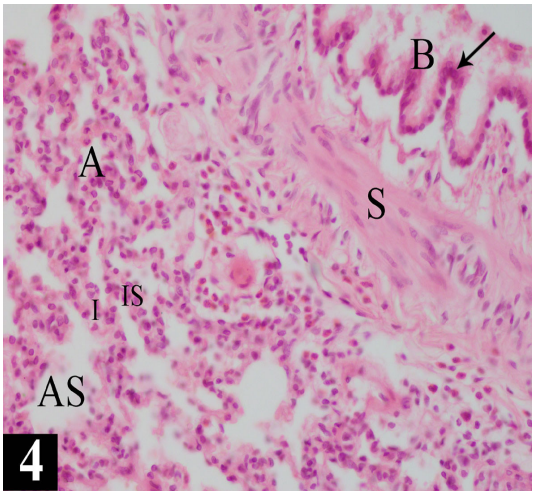

Fig. 4: A photomicrograph of a section in the lung of group II showing collapsed alveolar saccule (AS) and alveoli (A). The collapsed alveoli are separated by thickened interalveolar septa (IS). Pronounced cellular infiltration is noticed (I). Note a respiratory bronchiole (B) which is lined by respiratory epithelium (arrow) and surrounded by apparently thickened layer of smooth muscle (S). H & E, X400.

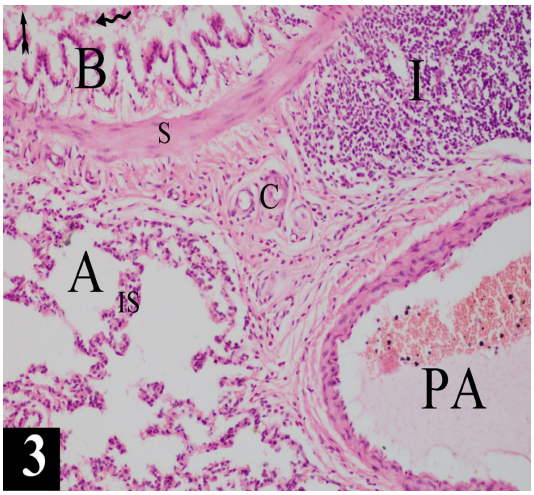

Fig. 3: A photomicrograph of a section in the lung of group II showing an alveolus (A) with thickened interalveolar septa (IS), dilated congested branch of pulmonary artery (PA), dilated congested blood capillaries (C) and a respiratory bronchiole (B) with surrounding thickened layer of smooth muscle (S). Intrabronchial cellular debris (wavy arrow) associated with RBCs (tailed arrow) are also observed. Note inflammatory cellular infiltration (I). H & E, X200.

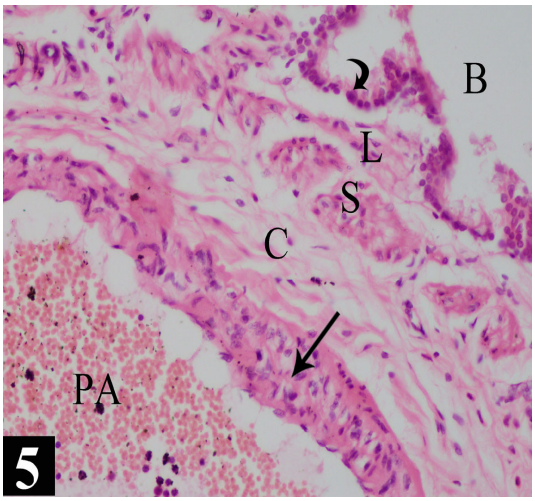

Fig. 5: A photomicrograph of a section in the lung of group II showing a respiratory bronchiole (B) which is lined by a non-ciliated Clara cell (curved arrow) and surrounded by lamina propria (L) under the bronchiolar epithelium, apparently thickened smooth muscle layer (S) and connective tissue (C). Note dilated congested branch of pulmonary artery (PA) with thickened wall (arrow). H & E, X400.

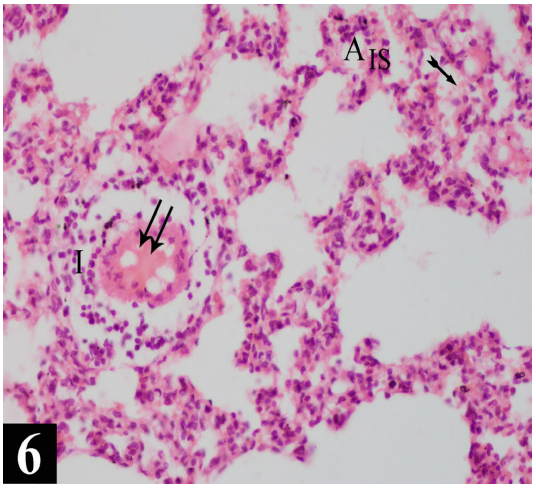

Fig. 6: A photomicrograph of a section in the lung of group II showing collapsed alveoli (A) which are separated by thickened interalveolar septa (IS). Inflammatory cellular infiltration (I), exudation (double arrow) and extravasated red blood cells within the alveolar lumen (tailed arrow) are noticed. H & E, X400.

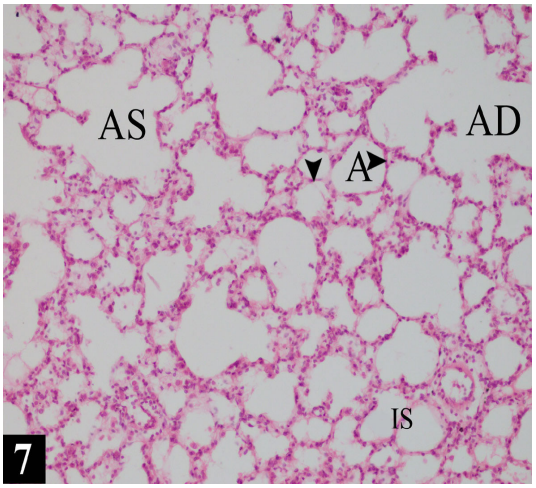

Fig. 7: A photomicrograph of a section in the lung of group III showing nearly normal structure of the alveolar duct (AD), alveolar saccule (AS) and alveolus (A) which is lined by simple squamous epithelium (arrow heads). The interalveolar septa appear relatively thin (IS). H & E, X200.

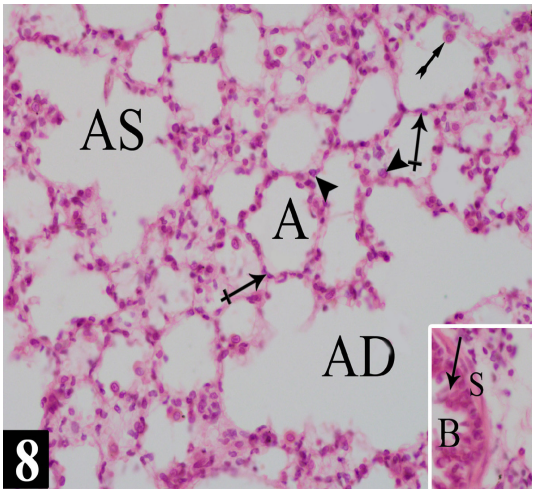

Fig. 8: A photomicrograph of a section in the lung of group III showing nearly normal structure of alveolar duct (AD), alveolar saccule (AS), alveolus (A) which is lined by flat pneumocytes type I (crossed arrows) and pneumocytes type II (arrow heads). Note alveolar macrophage (dust cell) (tailed arrow). H & E, X400. Inset: Showing a respiratory bronchiole (B) lined by respiratory epithelium (arrow). Note the surruounding smooth muscles which appear relatively thin (S). H & E, X400.

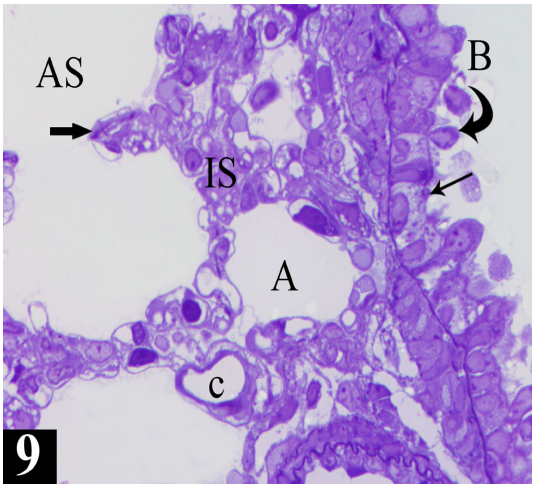

Fig. 9: A photomicrograph of a semithin section in the lung of a control rat showing normal structure of alveolar saccule (AS), alveolus (A) and interalveolar septa (IS). A normal bronchiole (B) lined by respiratory epithelium (arrow) and clara cell (curved arrow) is observed. Note short thin secondary septa (thick arrow) and a blood capillary (C). Toluidine blue, X1000.

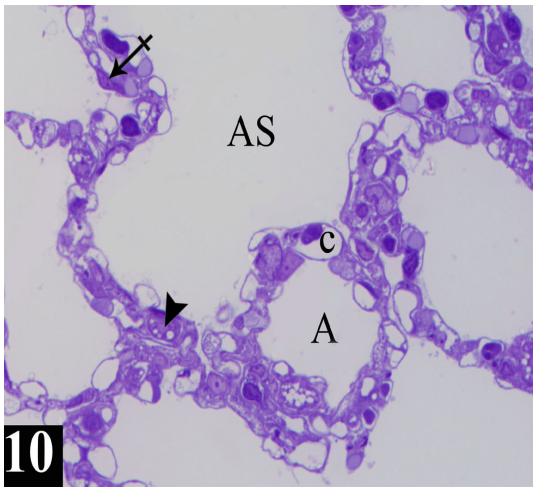

Fig. 10: A photomicrograph of a semithin section in the lung of a control rat showing normal structure of alveolar saccule (AS) and alveolus (A) which is lined by flat pneumocyte type I (crossed arrow) and few rounded pneumocyte type II (arrow head). A blood capillary (C) is seen. Toluidine blue, X1000.

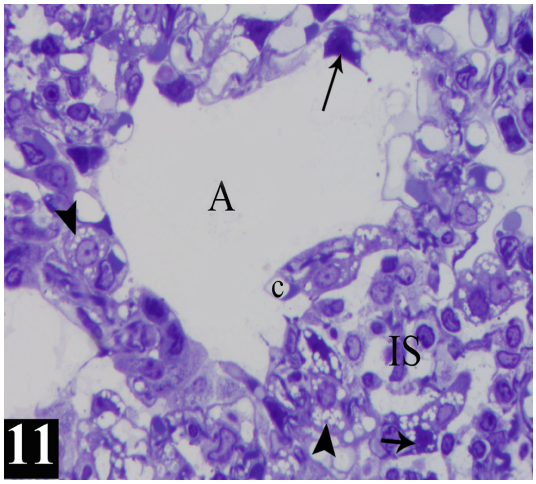

Fig. 11: A photomicrograph of a semithin section in the lung of group II showing abnormal alveolus (A) with thickened interalveolar septa (IS), degenerated cells (arrow) and pneumocyte type II (arrow heads) with markedly vacuolated cytoplasm. Numerous vacuolated cells with darkly stained irregular nuclei (short arrow) appear in the thickened interalveolar septa. Many blood capillaries (C) can be seen facing the alveolar lumen and the tips of secondary septa. Toluidine blue, X1000.

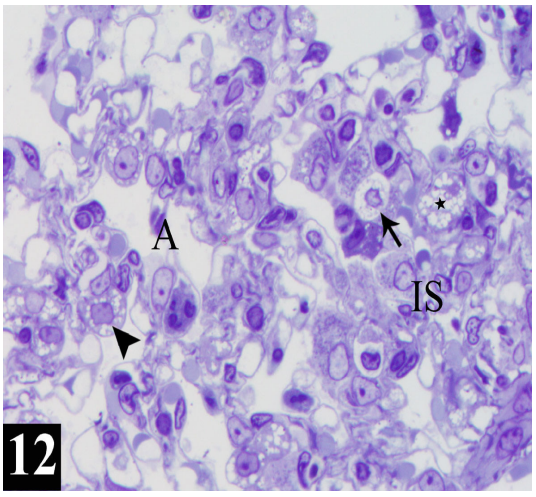

Fig. 12: A photomicrograph of a semithin section in the lung of group II showing a collapsed alveolus (A) which reveals pneumocyte type II (arrow head) with large irregular nuclei and maked cytoplasmic vacuolations. The thickened interalveolar septa (IS) contain cells with irregular nuclei and vacuolated cytoplasm (short arrow) and other cells with fragmented nuclei (asterisk). Toluidine blue, X1000.

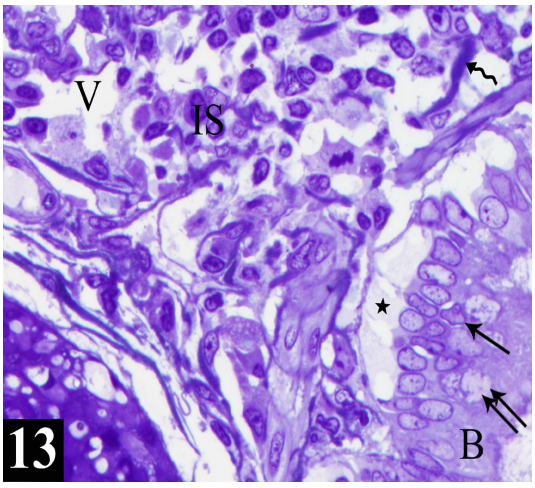

Fig. 13: A photomicrograph of a semithin section in the lung of group II showing a part of bronchiole (B) lined by respiratory epithelium (arrow) and goblet cells (double arrow). Separation of the epithelium from its underlying basement membranes is observed in some bronchioles (asterisk). Note the thickened interalveolar septa (IS) which contain many vacuolated areas (V) and areas of degenerations (wavy arrow). Toluidine blue, X1000.

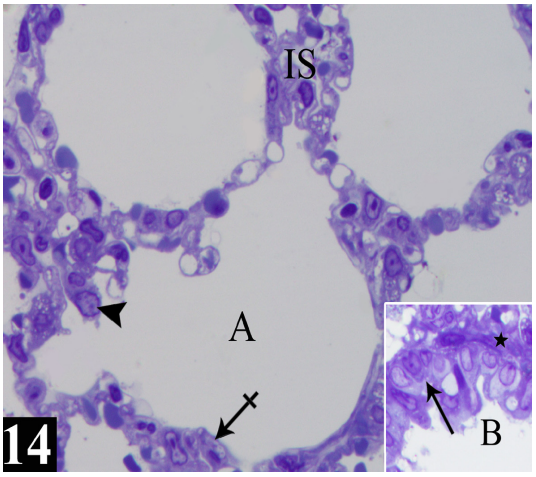

Fig. 14: A photomicrograph of a semithin section in the lung of group III showing nearly normal alveolus (A) lined by a flat pneumocyte type I (crossed arrow) and a pneumocyte type II (arrow head). Note relatively thin interalveolar septa (IS). Toluidine blue, X1000. Inset: Showing a part of bronchiole (B) lined by respiratory epithelium (arrow). The bronchial wall revealed relatively maintained continuity with the underlying basement membrane (asterisk). Toluidine blue, X1000.

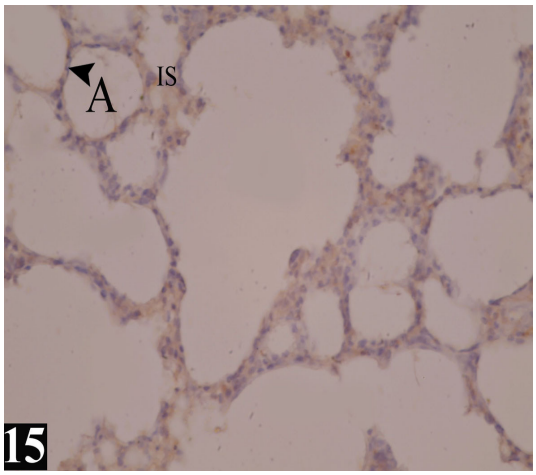

Fig. 15: A photomicrograph of a section in the lung of a control rat showing a negative cytoplasmic immune reaction for caspase-3 along the lining epithelial cells (arrow head) of alveolar wall (A) and in the interalveolar septa (IS). Caspase-3, X400.

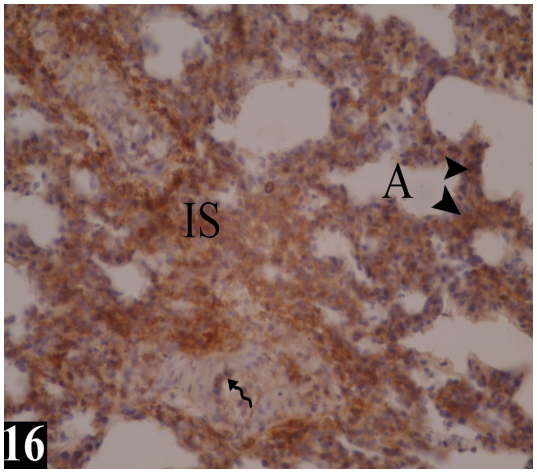

Fig. 16: A photomicrograph of a section in the lung of group II showing an intense brownish cytoplasmic immune reaction for caspase-3 along the lining epithelial cells (arrow heads) alveolar of wall (A), interalveolar septa (IS) and along the endothelial lining of some blood vessels (wavy arrow). Caspase-3, X400.

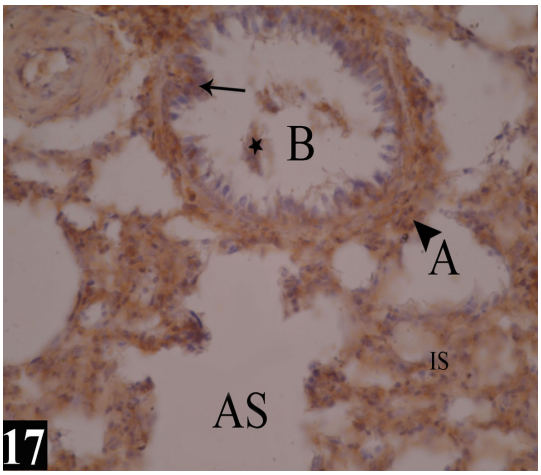

Fig. 17: A photomicrograph of a section in the lung of group II showing a strong brownish cytoplasmic immune reaction for caspase-3 in the lining epithelial cells (arrow) of bronchiole (B), lining epithelium (arrow head) of alveoli (A) and interalveolar septa (IS) and along the exfoliated bronchial epithelial cells (asterisk). Note the alveolar saccule (AS). Caspase-3, X400.

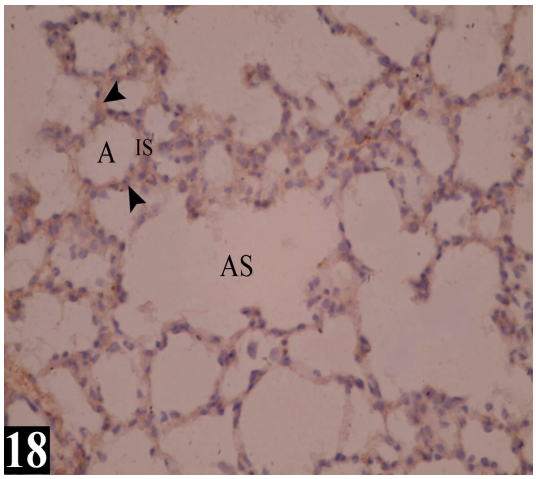

Fig. 18: A photomicrograph of a section in the lung of group III showing a slight cytoplasmic immune reaction for caspase-3 along the lining epithelial cells (arrow heads) of alveolar wall (A) and interalveolar septa (IS). Note the alveolar saccule (AS). Caspase-3, X400.

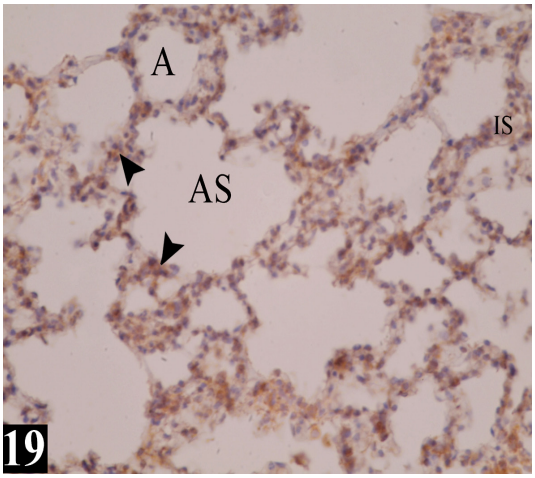

Fig. 19: A photomicrograph of a section in the lung of a control rat showing a weak immune reaction to inducible nitric oxide synthase (iNOS) in the lining epithelial cells (arrow heads) of alveolar wall (A), alveolar saccule (AS) and along the interalveolar septa (IS). iNOS, X400.

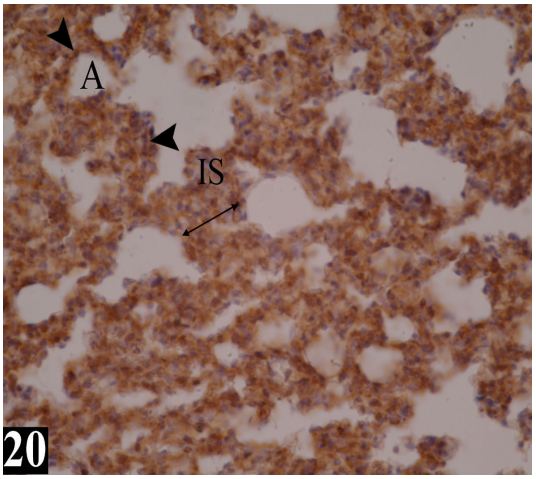

Fig. 20: A photomicrograph of a section in the lung of group II showing an intense iNOS expression as a brown cytoplasmic immune reaction in the interalveolar septa (IS) wthich appear thickened (↔) and along the epithelium (arrow heads) of alveolar wall (A). iNOS, X400.

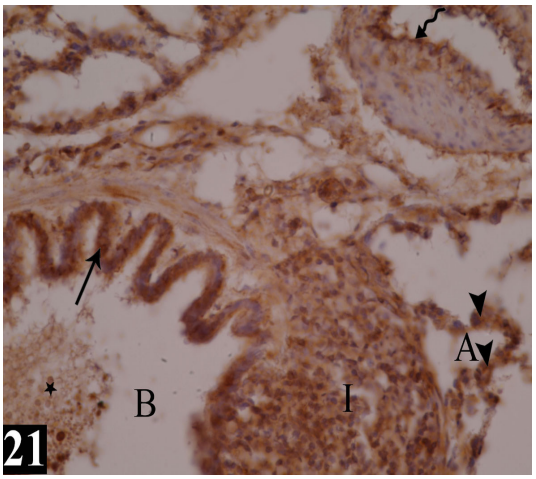

Fig. 21: A photomicrograph of a section in the lung of group II showing a strong iNOS expression in the lining epithelial cells (arrow) of bronchiole (B), exfoliated bronchial epithelial cells (asterisk), lining epithelial cells (arrow heads) of alveoli (A) and along the endothelial lining of some blood vessels (wavy arrow). Note a strong iNOS expression among an area of inflammatory cellular infiltration (I) (remove white arrow). iNOS, X400.

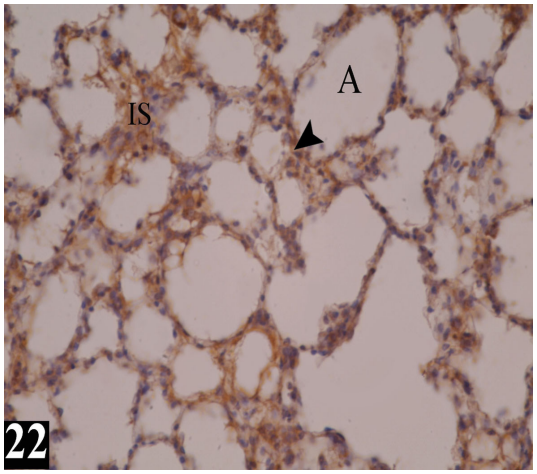

Fig. 22: A photomicrograph of a section in the lung of group III showing moderate iNOS expression in the lining epithelial cells (arrow head) of alveoli (A) and among the interalveolar septa (IS). iNOS, X400.

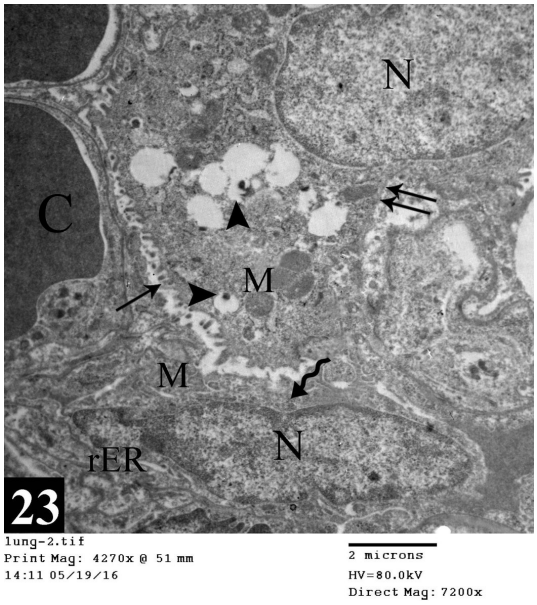

Fig. 23: An electron micrograph of a section in the lung of a control rat showing a pneumocyte type – I (wavy arrow). The cell has a flat nucleus (N) and is surrounded by a narrow perinuclear cytoplasm containing mitochondria (M) and rough endoplasmic reticulum (rER). A part of pneumocyte type II (double arrow) with a large nucleus (N) is also detected. Its cytoplasm shows lamellar bodies (arrow heads) and mitochondria (M) with variable sizes and shapes. Short microvilli are observed on the cell surface (arrow). Note blood capillaries (C). TEM, X7200.

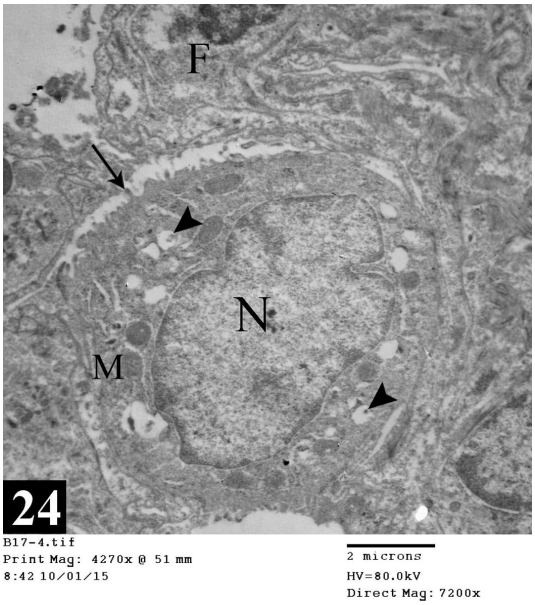

Fig. 24: An electron micrograph of a section in the lung of a control rat showing a pneumocyte type – II with a large euchromatic nucleus (N). The cytoplasm reveals lamellar bodies (arrow heads) and mitochondria (M) with variable sizes and shapes. The interstitial connective tissue contains a fibroblast (F). Note short microvilli (arrow) on the cell surface. TEM, X7200.

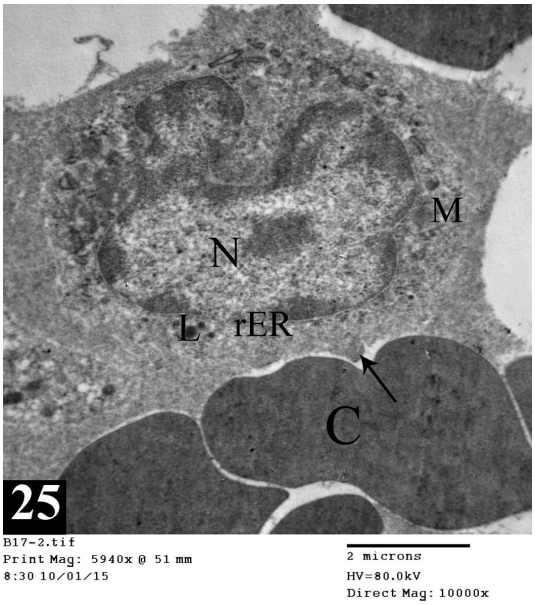

Fig. 25: An electron micrograph of a section in the lung of a control rat showing an alveolar macrophage with pseudopodia (arrow). The cell has a large indented nucleus (N) and many cytoplasmic lysosomes (L). Mitochondria (M) and rough endoplasmic reticulum (rER) can be seen. Note blood capillaries (C). TEM, X10,000.

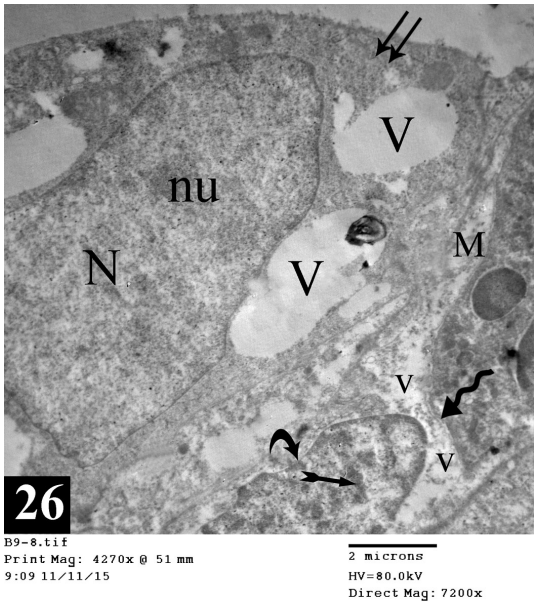

Fig. 26: An electron micrograph of a section in the lung of group II showing a pneumocyte type I (wavy arrow) with indentation of its nuclear membrane (curved arrow) and presence of chromatin clumps inside the nucleus (tailed arrow).The cytoplasm reveals marked vacuolations (v) and swollen mitochondria with disrupted cristae (M). A pneumocyte type II (double arrow) with a large nucleus (N) which has nucleolus (nu) is observed. The cell shows degenerative changes of its lamellar bodies leaving large irregular empty vacuoles (V). TEM, X7200.

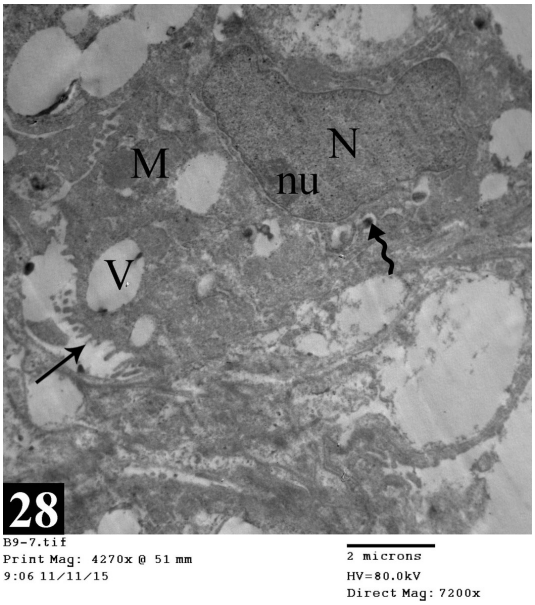

Fig. 28: An electron micrograph of a section in the lung of group II showing an electron-dense pneumocyte type II with vacuolated lamellar bodies (V). The nucleus (N) appears electron dense with a nucleolus (nu). The cytoplasm shows swollen electron dense mitochondria (M) and phagosomes (wavy arrow). Note the microvillous border (arrow). TEM, X7200.

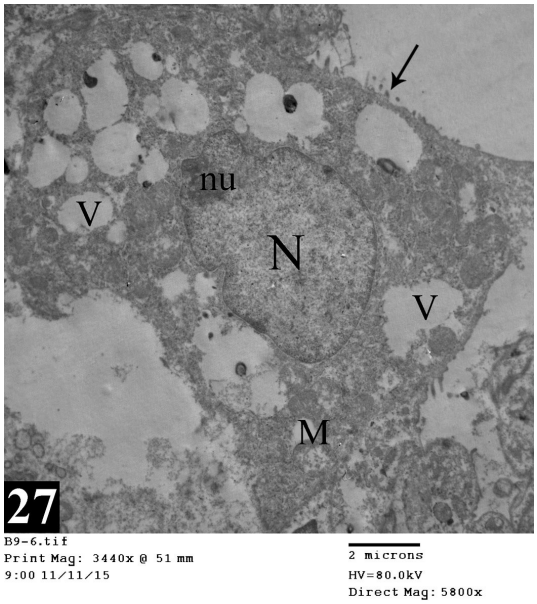

Fig. 27: An electron micrograph of a section in the lung of group II showing a pneumocyte type II recognized by its microvillous border (arrow). The cell has a large nucleus (N) with a nucleolus (nu). Numerous large vacuolated lamellar bodies (V) occupying a lage portion of the cytoplasm and swollen mitochondria with disrupted cristae (M) are noticed. TEM, X5800.

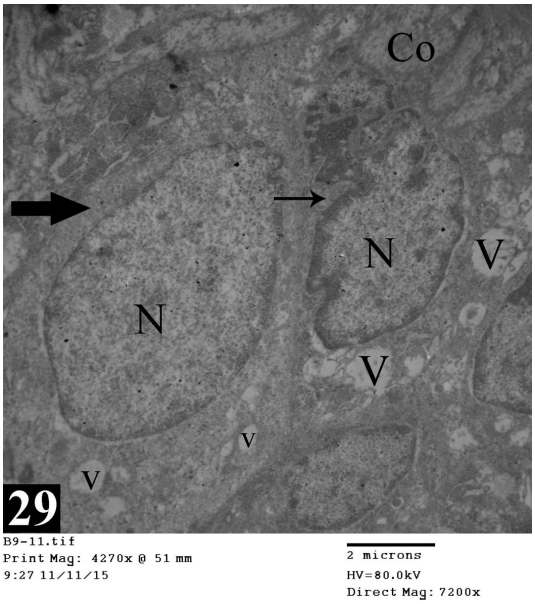

Fig. 29: An electron micrograph of a section in the lung of group II showing two adjacent pneumocytes type II. One cell (thin arrow) with a fragmented nucleus (N) and vacuolated lamellar bodies (V). The other cell (thick arrow) shows a large indented nucleus (N) and some cytoplasmic vacuoles (v). Interstitial collagen fibers (Co) are also observed. TEM, X7200.

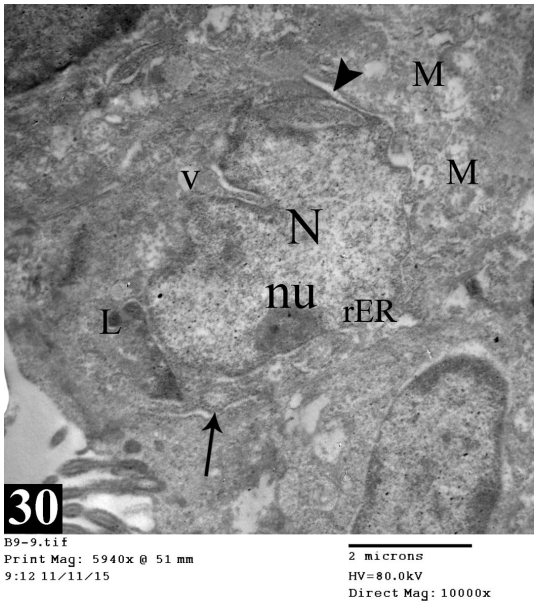

Fig. 30: An electron micrograph of a section in the lung of group II showing an alveolar macrophage with pseudopodia (arrow) and a large indented nucleus (N) which contains a nucleolus (nu). Dilated perinuclear cisternae (arrow head) can be seen. The cytoplasm reveals swollen mitochondria with disrupted cristae (M), lysosomes (L) and many cytoplasmic vacuoles (V). Note dilated rough endoplasmic reticulum (rER). TEM, X10,000.

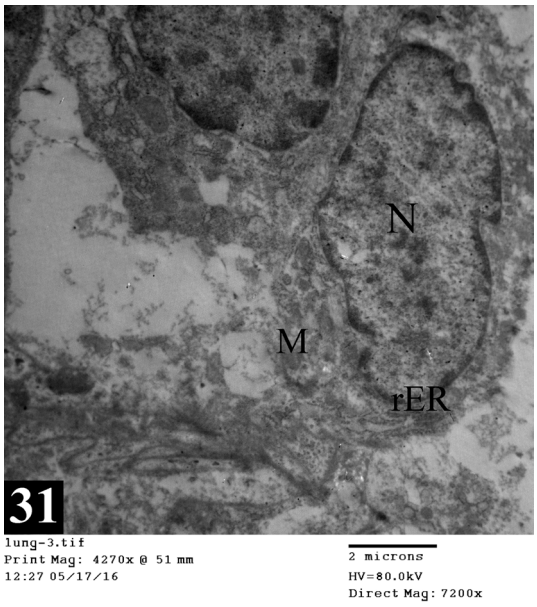

Fig. 31: An electron micrograph of a section in the lung of group III showing a pneumocyte type – I with a flat nucleus (N) and surrounding narrow perinuclear cytoplasm. Mitochondria (M) and rough endoplasmic reticulum (rER) can be noticed inside the cytoplasm. TEM, X7200.

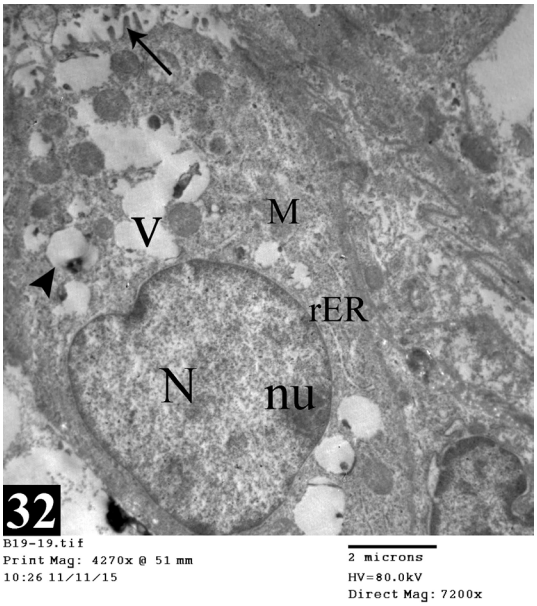

Fig. 32: An electron micrograph of a section in the lung of group III showing an euchromatic nucleus (N) and a nucleolus (nu) of pneumocyte type – II. The cytoplasm reveals lamellar bodies either containing secretions (arrow head) or empty (V), rough endoplasmic reticulum (rER) and mitochondria (M) which appear healthy with variable sizes. Note short microvilli on the cell surface (arrow). TEM, X7200.

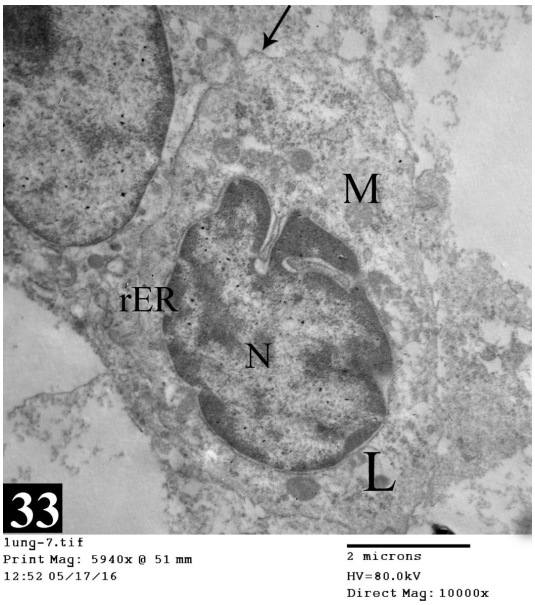

Fig. 33: An electron micrograph of a section in the lung of group III showing an alveolar macrophage which has pseudopodia (arrow). The nucleus (N) appears large and indented. Mitochondria (M), lysosomes (L) and rough endoplasmic reticulum (rER) can be observed inside the cytoplasm. TEM, X10,000.

DISCUSSION

In the current study, the light microscopic examination of rat lungs after immobilization revealed severe alveolar damage in the form of collapsed alveolar saccule and alveoli, markedly thickened interalveolar septa encroaching on alveoli and heavy inflammatory cellular infiltration and exudation. Degenerated cells and cells with irregular or fragmented nuclei and vacuolated cytoplasm can be noticed. Respiratory bronchioles showed exfoliation of many cells from their lining epithelium and cellular debris in their lumina associated with RBCs. The structural changes that occured in the lungs after immobilization in this work were similar to changes seen after some other forms of shock and stress, including the respiratory distress syndrome in human infants (*Harrison et al., 1969; Adamson et al., 1970; Rathff et al., 1970; Moss, 1972; Moss et al., 1972; Connell et al., 1975; Caddell et al., 1987*).

It has been demonstrated that some forms of stress, such as exercise, starvation, trauma, major surgery, radiation, emotional and oxidation stress, increase the free radical generation with subsequent initiation of lipid peroxidation. Free radical oxidation of unsaturated lipids has a role in a variety of pathological conditions. The free radical processes play a role in the control of general physiological response to stress. Many studies confirm involvement of free radical processes, mainly lipid peroxidation, in different stages of stress (*Kovacheva-Ivanova et al., 1994*).

Liu and Mori (1994) examined the oxidative damage and antioxidant defense changes with immobilization-induced emotional stress in the rat brain. They found that immobilization stress may induce the formation of reactive oxygen species (ROS) which weakens the brain antioxidant defenses and induces an oxidative damage. The antioxidant administration of reduced glutathione provides further evidence to support the above hypothesis. ROS are involved in the pathogenesis of many diseases and pathologic processes and play an important part in the complex physiological processes such as apoptosis. Cellular injury caused by ROS is associated with their impact on cellular structure (membrane lipoperoxidation, DNA strand breaks) and function (changes in the enzymatic activity, signalling) (*Tkaczyk and Vizek, 2007*).

Tkaczyk and Vizek (2007) suggested that lung is one of the organs commonly affected by ROS generation. The lung has a large surface that is constantly in contact with air oxygen and pollutants. So, it is a site of major ROS production. This has lead to the evolution of an antioxidant defence system to protect the lungs from substantial damage. When the balance between ROS production and the defensive capacity of the antioxidant system is disturbed, pathological reactions may cause injury or disease. They added that the possible cellular sources of ROS in the lungs are neutrophils, eosinophils, alveolar macrophages, peripheral monocytes-macrophages attracted by inflammatory cytokines which contribute to the damage in pulmonary diseases, mast cells, type II pneumocytes, endothelial cells, smooth muscle cells and lung fibroblasts. During inflammation phagocytes are the main source of the oxidative stress.

In line with the present results, *Capelozzi et al. (2007)* showed that swimming-induced stress amplified mononuclear cell recruitment to the lungs in guinea pigs that were subjected to that stress. Few studies have been dedicated to analyze the effects of emotions and stress on distal airway inflammation and remodeling. The study of *Leick et al. (2012)* revealed that repeated stress, induced by repeated forced swim, amplified distal airway responsiveness to antigen challenge, which was associated with an increase in lymphocytes and eosinophils in distal airways. *Almeida-Reis et al. (2010)* showed that animals subjected to the repeated forced swim stress had greater values of serum cortisol and adrenal weight compared to non-stressed groups. *Portela et al. (2002)* observed that sensitized and stressed rats had an enhancement of airway edema and lymphocytic infiltration. In accordance, *Capelozzi et al. (2007)* found an enhancement of eosinophilic density on the alveolar wall in stressed guinea pigs. In humans, *Liu et al. (2002)* analyzed the effects of low stress or a stress phase in college students with mild asthma. They found that the number of sputum eosinophils was increased during the stress phase. *McEwen (2000) and Sapolsky et al. (2000)* recorded that many substances produced during the stress responses modulated eosinophilic recruitment and apoptosis.

Nuclear factor κB (NF-κB) is a redox-sensitive transcription factor responsive to

closely related reactive oxygen species (ROS) and reactive nitrogen species (RNS) redox cascades. Several studies have demonstrated its involvement in exercise and immobilization, indicating that these conditions may lead to inflammatory responses and to oxidative damage to tissues. Recent studies have proved that NF-κB is involved in inflammatory responses that may result in muscle protein degradation (*Bar-Shai et al., 2008*).

Kovacheva and Ribarov (1995) explained the damaging effect of immobilization stress by the fact that the lung and the pulmonary vasculature are at high risk of injury mediated by oxygen-derived free radicals and lipid peroxidation. This due to the fact that lung tissue contains unsaturated fatty acids, which considered as a substrate of lipid peroxidation, and the lung is exposed to higher concentrations of oxygen than any other organ in the body. Nevertheless, in normal conditions, the level of lipid peroxidation in the lung is very low, because of the powerful antioxidant systems of the lung.

In the present work, an intense cytoplasmic immune reaction for caspase-3 was found in the lining epithelial cells of bronchiole, alveoli, interalveolar septa, endothelial lining of some blood vessels and along the exfoliated bronchial epithelial cells in the stressed group compared with the control group. In harmony with the present findings, *Porter and Jänicke (1999)* suggested that Caspase-3 has been found to be necessary for normal brain development as well as its typical role in apoptosis, where it is responsible for chromatin condensation and DNA fragmentation. Caspase-3 is activated in the apoptotic cell both by extrinsic (death ligand) and intrinsic (mitochondrial) pathways (*Salvesen, 2002; Ghavami et al., 2009*).

The current study revealed strong iNOS expression as brown cytoplasmic reaction in the lining epithelial cells of bronchioles, alveoli, endothelium of bronchiolar arterioles, cells of thickened interalveolar wall and among an area of inflammatory cellular infiltration suggested inflammatory process. In agreement with the present results, *Leick et al. (2012)* reported that in the same animal model, a repeated forced swimming stressor increased lung distal constriction. These responses were associated with an increase in actin content, inducible nitric oxide synthase expression and oxidative stress pathway activation, suggesting that nitric oxide contributes to pulmonary stress-induced structural and functional alterations. *Kobzik et al. (1993)* localized iNOS in fixed tissue of rat and human lung. They found that immunoreactive iNOS was most apparent in rat alveolar macrophage, occasionally in human macrophage and endothelium in areas of chronic inflammation. In accordance, *Antošová et al. (2015)* reported that iNOS, which produces large amounts of Nitric oxide (NO), is active during the inflammatory process. Nitric oxide effects in airways are influenced by the activity of NO-synthase isoforms and NO metabolism. NO quickly reacts, producing ROS.

In the present study, the ultrastructure of lung sections of the stressed rats showed damaged pneumocytes type I&II. Some cells revealed indentation of the nuclear membrane and presence of chromatin clumps inside the nucleus. Swollen mitochondria with disrupted cristae and cytoplasmic vacuolations were observed. Vacuolated lamellar bodies which were relatively deprived of their content of secretory surfactant material leaving irregular empty spaces associated with collagen fiber deposition can be noticed in pneumocyte type II. Many cells showed an apparent increase in the size of their lamellar bodies which appeared more frequent when compared with the control group. Some cells appeared electron dense with electron dense nucleus, phagosomes and swollen electron dense mitochondria. Other cells showed fragmented nucleus. Numerous collagen fibers deposited in the interstitium were noticed. Many large macrophages with dilated rough endoplasmic reticulum, swollen mitochondria with disrupted cristae, phagosomes and dilated perinuclear cisternae were present in the alveolar spaces and in the lung interstitium.

In harmony with the present findings, *Kovacheva-Ivanova et al. (1994)* found that the ultrastructure of rat lungs after immobilization revealed progressive damage to the alveolar wall, with acute inflammatory reaction and development of oedema being the initial stages of this process. They reported that alveolar type I cells are affected first, followed by alveolar type II cell. In accordance, histopathological changes were induced in stomach, intestine, testis and adrenal gland under immobilization stress in male rats *(Gabry et al., 2002; El-Refaiy, 2010;*

El-Desouki et al., 2011). The present results can be explained by *Li u et al. (1996)* who reported reduction in total protein and concluded that immobilization stress caused oxidative damage to protein in rat. Also, *Sakr and El- Abd (2009)* recorded significant reduction of proteins in spermatogenic cells of rat testes exposed to oxidative stress and the same was reported by *El-Refaiy (2010)* in rat testes by immobilization stress for different durations. Moreover, the reduction in total protein was demonstrated in rat adrenal cortical cells under immobilization stress ultrastructurally *(El-Desouki et al., 2011)* and in gastric mucosa *(Nagi, 2012)*.

Bagchi et al. (1999) and Rai et al. (2003) found that exposure to stress can lead to increased production of free radicals that contribute to the occurrence of pathological conditions through stimulation of numerous pathways. *Ganesan et al. (2011)* reported that restraint stress may lead to oxidative damage through impairment the antioxidant defence system, by changing the balance between oxidant and antioxidant factors. Malonaldhyde level (a biomarker of lipid peroxidation) was also increased significantly while glutathione level (a biomarker of protective oxidative injury) was significantly decreased in all tissues after exposure to stress *(Erosy et al., 2008)*. The mechanism underlying the induction of lipid peroxidation in lung cell membranes during immobilization stress can be explained by the fact that lipid peroxidation may be triggered by the stress-induced high levels of plasma catecholamines *(Haggendal et al. 1987)*; the release of transition metal complexes from various storage sites *(Packer 1985; Halliwell and Gutteridge 1989)* and the development of hypoxia and metabolic acidosis *(Poyarov et al. 1990)*. Moreover, *Kovacheva-Ivanova et al. (1994)* suggested that lipid peroxidation is the cause, rather than the consequence of the lung structure damage. According to the results of *Şahin and Gümüşlü (2007)*, it was concluded that immobilization stress may lead to increment of free radical generation which may have changed antioxidant enzyme activities, and cause protein oxidation and lipid peroxidation of tissues.

The melatonin-treated stressed group in the current study showed an improvement of histological structure of alveoli, alveolar ducts, saccules, interalveolar connective tissue wall and alveolar macrophages (dust cells). Also, the cytoplasmic immune reaction for caspase-3 and iNOS expression in the lining epithelial cells of alveoli, alveolar saccules and interalveolar wall showed marked reduction. The ultrastructure showed nearly normal structure of type-I and type-II pneumocytes. These improvements can be explained by the fact that every cell is endowed with mechanisms protecting it against the damaging effects of ROS. Antioxidants are recognized both intra- and extracellular and divided into enzymatic and non-enzymatic categories as well. They were classified as primary (preventing oxidant formation), secondary (scavenging ROS) and tertiary (removing or repairing oxidatively modified molecules) which may be constitutive, inducible or dietary according to their origin *(Gutteridge and Halliwell, 2000)*. *Comhair and Erzurum (2002)* found that the lung is directly exposed to the environment and to oxygen at higher partial pressure than other organs; its antioxidant defence is, therefore, particularly important.

The present findings were also supported by *Farias et al. (2012)* who demonstrated that melatonin plays a protective role in the heart, lung and kidney in animals exposed to lipid peroxidation which results in a lower malonydialdehyde content in such tissues. *Ishii et al. (2009)* and *Sanchez-Hidalgo et al. (2009)* reported that melatonin membrane receptors like MT1 and MT2 have been described in heart, lung, liver and kidney. Other investigators observed the cytoprotective effects of melatonin on different stress and inflammatory models on the GIT *(Kato et al., 2002)*. Also, *Othman et al. (2001)*; *Bandyopadhyay et al. (2002)* and *Bilici et al. (2002)* suggested that melatonin pretreatment decreased gastric mucosal lesions and inhibited the generation of free oxygen radicals in restraint-cold stress treated rats. Melatonin treatment ameliorated these alterations via its antioxidant effect in all these models.

Serel et al. (2004); Kucukakin et al. (2009) and *Gitto et al. (2011)* proved that melatonin is a highly effective antioxidant, scavenging hydroxyl radicals and inhibiting the production of nitric oxide and other antioxidants like vitamins E and C. The ability of melatonin to counteract ROS formation is due to the special characteristic of this substance to cross morpho and physiological barriers distributed in tissues, cells and subcellular compartments due to its

distinct physical and chemical properties *(Costa et al., 1995; Tomas-Zapico and Coto-Montes, 2005)*. In addition, melatonin also can exhibit strong direct and indirect antioxidant properties, one of which is direct capturing of ROS and another is stimulating gene expression and the activity of some enzymes that can activate enzymatic antioxidants *(Kücükakin et al., 2009)*.

CONCLUSION

The immobilization stress induced a damaging effect on the histological structure of the lung and a concomitant administration of melatonin effectively protected the lung tissue.

REFERENCES

Abd-Allah, A.R., El-Sayed, S.M., Abdel-Wahab, M.H. and Hamada, F.M. 2003. Effect of melatonin on estrogen and progesterone receptors in relation to uterine contraction in rats. Pharmacological Research, 47:349-354.

Adamson, I.Y.R., Bowden, D.H. and Wyatt, J.P. 1970. A pathway to pulmonary fibrosis An ultrastructuial study of mouse and rat following radiation to the whole body and hemithorax Amer. Journal of Pathology, 58:481- 498.

Almeida-Reis, R., Toledo, A.C., Reis, F.G., Marques, R.H., Prado, C.M., Dolhnikoff, M., Martins, M.A., Leick-Maldonado, E.A. and Tibério, I.F. 2010. Repeated stress reduces mucociliary clearance in animals with chronic allergic airway inflammation. Respiratory, Physiology and Neurobiology, 173: 79–85.

Antošová, M.1., Strapková, A., Mikolka, P., Mokrý, J., Medvedová, I. and Mokrá, D. 2015. The influence of L-NAME on iNOS expression and markers of oxidative stress in allergen-induced airway hyperreactivity. Advances in Experimental Medicine and Biology, 838:1-10.

Bagchi, D., Carryl, O.R., Tran, M.X., Bagchi, M., Garg, A., Milnes, M.M., Williams, C.B., Balmoori, J., Bagchi, D.J., Mitra, S. and Stohs, S.J. 1999. Acute and chronic stress-induced oxidative gastrointestinal mucosal injury in rats and protection by bismuth subsalicylate. Mol. Cell Biochem. 196 (1-2): 109-116.

Bancroft, J.D. and Gamble, M. 2002. Theory and practice of histological techniques. 5th ed. Churchill Livingstone, Philadelphia.

Bancroft, J.D. and Gamble, M. 2007. Theory and practice of histological techniques. 6th ed. Churchill Livingstone, London; 179.

Bandyopadhyay, D., Bandyopadhyay, A., Das, P.K. and Reiter R.J. 2002. Melatonin protects against gastric ulceration and increases the efficacy of ranitidine and omeprazole in reducing gastric damage. Journal of Pineal Research 33 (1):1–7.

Barriga, C., Martin, M.I., Tabla, R., Ortega, E. and Rodriges, A.B. 2001. Circadian rhythm of melatonin, corticosterone and phagocytosis: Effect of stress. Journal of Pineal Research 30:180−187.

Bar-Shai, M; Carmeli, E; Ljubuncic, P. and Reznick, A.Z. 2008. Exercise and immobilization in aging animals: The involvement of oxidative stress and NF-κB activation. Free Radical Biology and Medicine 44 (2): 202–214

Bassani, T.B., Gradowski, R.W., Zaminelli, T., Barbiero, J.K., Santiago, R.M., Boschen, S.L., da Cunha, C., Lima, M.M., Andreatini, R. and Vital, M.A. 2014. Neuroprotective and antidepressant-like effects of melatonin in a rotenone-induced Parkinson's disease model in rats. Brain Research, 17:95-105.

Bertsch, K., Schmidinger, I., Neumann, I.D. and Herpertz, S.C. 2013. Reduced plasma oxytocin levels in female patients with borderline personality disorder. Hormones and Behavior, 63:424-429.

Bian, J.S.,Wang, Y.L. and Li, D.X. 1997. Immobilization stress induced changes of ventricular electric stability in damaged heart depends on the extent of free radical damage. Shengli Xuebao 49:526–530.

Bilici, D., Suleyman, H., Banoglu, Z.N., Kiziltunç, A., Avci, B., Çiftçioğlu, A. and Bilici, S. 2002. Melatonin prevents ethanol-induced gastric mucosal damage possibly due to its antioxidant effect. Digestive Diseases and Sciences 47:856–861.

Caddell, J.L., Blanchette-Mackie, E.J., Snowden, K.I. and Jackson, N.N. 1987. Pulmonary lesion induced by stress m magnesium-deficient rats: A light and electron

microscopic study. American Journal of Pathology, 127:430-440.

Capelozzi, M.A., Leick-Maldonado, E.A., Parra, E.R., Martins, M.A., Tiberio, I.F. and Capelozzi V.L. 2007. Morphological and functional determinants of fluoxetine (Prozac)-induced pulmonary disease in an experimental model. Respiratory, Physiology and Neurobiology, 156: 171–178.

Carloni, S., Perrone, S., Buonocore, G., Longini, M., Proietti, F. and Balduini W. 2008. "Melatonin protects from the long-term consequences of a neonatal hypoxic-ischemic brain injury in rats." Journal of Pineal Research 44 (2): 157–164.

Comhair, S.A. and Erzurum, S.C. 2002. Antioxidant responses to oxidant-mediated lung diseases. American journal of physiology. Lung cellular and molecular physiology, 283: 246–255.

Connell, R.S., Swank, R.L. and Webb, M.C., 1975. The development of pulmonary ultrastructural lesions during hemorrhagic shock. Journal of Trauma 15:116-129.

Costa, E.J., Lopes, R.H. and Lamy-Freund, M.T. 1995. Permeability of pure lipid bilayers to melatonin. Journal of Pineal Research. 19:123–126.

Demling, R.H., Lalonde, C., Jin, L.J., Ryan, P. and Fox, R. 1986. Endotoxemia causes increased lung tissue lipid peroxidation in unanesthetized sheep. Journal of applied Physiology, 60(6): 2094-2100.

Dhabhar, F.S. and McEwen, B.S. 1999. Enhancing versus suppressive effects of stress hormones on skin immune function. Proceedings of the National Academy of Sciences of the United States of America, 96: 1059–1064.

Dragoş, D. and Tănăsescu, M.D. 2010. The effect of stress on the defense systems. Journal of Medicine and Life. 3(1): 8-10.

El-Desouki, N.I., El-Refaiy, A.I., Abdel-Azeem, H. and El-Baely, M.A. 2011. Histological and ultrasructural studies of the effect of immobilization stress on the adrenal cortex of albino rat and the ameliorative role of diazepam. Journal of the Egyptian German Society of Zoology 62: 25- 45.

El-Refaiy, A.I. 2010. Histological and histochemical studies on the testes of albino rat under immobilization stress and the possible curative role of diazepam. Journal of the Egyptian German Society of Zoology 60: 1-22.

Erosy, Y., Çikler, E., Çetinel, S., Sener, G. and Ercan, F. 2008. Leukotriene D4 receptor antagonist montelukast alleviates water avoidance stress-induced degeneration of the gastrointestinal mucosa. Prostaglandins. Leukotrienes and Essential Fatty Acids. 78(3):189 -197.

Farías, J.G., Zepeda, A.B. and Calaf, G.M. 2012. Melatonin Protects the Heart, Lungs and Kidneys from Oxidative Stress under Intermittent Hypobaric Hypoxia in Rats. Biological Research. 45: 81-85.

Fulia, F., Gitto, E., Cuzzocrea, S., Reiter, R.J., Dugo, L., Gitto, P., Barberi, S ., Cordaro, S. and Barberi, I. 2001. "Increased levels of malondialdehyde and nitrite/nitrate in the blood of asphyxiated newborns: reduction by melatonin," Journal of Pineal Research 31(4): 343–349.

Gabry, K.E., Chrousos, G.P., Rice, K.C., Mostafa, R.M., Sternberg, E., Negrao, A.B., Webster, E.L., McCann, S.M. and Gold, P.W. 2002. Marked suppression of gastric ulcerogensis and intestinal responses to stress by a novel class of drugs. Journal of Molecular Psychiatry. 7(5): 474-483.

Ganesan, B., Anandan, R. and Lakshmanan, P.T. 2011. Studies on the protective effects of betaine against oxidative damage during experimentally-induced restraint stress in Wistar albino rats. Cell Stress Chaperones. 16 (6): 641-652.

Ghavami, S., Hashemi, M., Ande, S.R., Yeganeh, B., Xiao, W., Eshraghi, M., Bus, C.J., Kadkhoda, K., Wiechec, E., Halayko, A.J. and Los, M. 2009. "Apoptosis and cancer: mutations within caspase genes". Journal of Medical Genetics. 46 (8): 497–510.

Giralt, M., Gasull, T., Hernandez, J., Garcia, A. and Hidalgo, J. 1993. Effect of stress, adrenolectomy and changes in glutathione metabolism on rat kidney metallothionein content: comparison with liver metallothionein. BioMetals 6:171–178.

Gitto, E., Pellegrino, S., Gitto, P., Barberi, I., and Reiter, R.J. 2009. "Oxidative stress of the newborn in the pre- and postnatal period and the clinical utility of melatonin." Journal of Pineal Research 46 (2): 128–139.

Gitto, E., Aversa, S., Reiter, R.J., Barberi, I. and Pellegrin, S. 2011. Update on the use of melatonin in pediatrics. Journal of Pineal Research 50 (1): 21–28.

Gumuslu, S., Sarikcioglu, S.B., Sahin, E., Yargicoglu, P. and Agar, A. 2002. Influences of different stress models on the antioxidant status and lipid peroxidation in rat erythrocytes. Free Radical Research. 36:1277–1282.

Gutteridge, J.M.C. and Halliwell, B. 2000. Free radicals and antioxidants in the year 2000. A historical look to the future. Annals of the New York Academy of Sciences. 899:136-147.

Haggendal, J., Jonsson, L., Johansson ,G., Bjurstrom, S., Carlsten, J. and Thoien-Tolling, K. 1987. Catecholamme-induced free radicals in myocaidial cell necrosis on experimental stress m pigs Acta Physiologica and Scandinavica. 131, 447-452.

Halliwell ,B. and Gutteridge, J.M.C. 1989. Free Radicals in Biology and Medicine, 2nd ed. Clarendon Press, Oxford, UK.

Harrison, L.H., Bellei, J.J., Hinshaw, L.B., Coalson, J.J. and Greenfield, L.J. 1969. Effects of endotoxin on pulmonary capillary permeability, ultrastructure, and surfactant. Surgery, Gynecology and Obstetrics. 129: 723-733.

Hayat, M.A. 2000. Principles and techniques of electron microscopy: biological applications. 4th ed. Edinburgh, UK: Cambridge University Press; 37–59.

Hidalgo, J., Campmany, L., Borras, M., Garvey, J.S. and Armario, A. 1988. Metallothionem response to stress m rats role m free radical scavenging. American Journal of Physiology. 255, L518-524.

Hoglund, C.O., Axen, J., Kemi, C., Jernelov, S., Grunewald, J., Muller-Suur, C., Smith, Y., Gronneberg, R., Eklund, A., Stierna, P. and Lekander, M. 2006. Changes in immune regulation in response to examination stress in atopic and healthy individuals. Clinical and Experimental Allergy 36(8): 982–992.

Ishii, H., Tanaka, N., Kobayashi, M., Kato, M. and Sakuma, Y. 2009. Gene structures, biochemical characterization and distribution of rat melatonin receptors. Journal of Physiological Sciences. 59: 37-47.

Jaggi, A.S., Bhatia, N., Kumar, N., Singh, N., Anand, P. and Dhawan R. 2011. A review on animal models for screening potential anti-stress agents. Neurological Sciences. 32(6): 993-1005.

Johnson, E.O., Kamilaris, T.C., Chrousos, G.P. and Gold, P.W. 1992. Mechanisms of stress: a dynamic overview of hormonal and behavioral homeostasis. Neuroscience and Biobehavioral Reviews. 16:115–130.

Kato, K., Murai, I., Asai, S., Takahashi, Y., Nagata, T., Komuro, S., Mizuno, S., Iwasaki, A., Ishikawaà, K. and Arakawa, Y. 2002. Circadian rhytm of melatonin and prostaglandin in modulation of stress-induced gastric mucosal lesions in rats. Alimentary Pharmacology and Therapeutics 16 (2):29–34.

Kiernan, J.A. 2001. Histological and histochemical methods: theory and practice. 3rd ed. A Hodder Arnold Publication, Oxford.

Kobzik, L., Bredt, D.S., Lowenstein, C. J., Drazen, J., Gaston, B., Sugarbaker, D. and Stamler, J.S. 1993. Nitric oxide synthase in human and rat lung: immunocytochemical and histochemical localization. American Journal of Respiratory. Cellular and Molecular Biology 9:371-377.

Kovacheva-Ivanova, S., Bakalova, R. and Ribarov, S.R. 1994. Immobilization Stress Enhances Lipid Peroxidation in the Rat Lungs. General Physiology and Biophysics. 13:469-482.

Kovacheva, S. and Ribarov, S. R. 1995. Lipid Peroxidation in Lung of Rat Stressed by Immobilization: Effects of Vitamin E Supplementation. Lung 173:255-263.

Kucukakin, B., Gogenur, I., Reiter, R.J. and Rosenberg, J. 2009. Oxidative Stress in Relation to Surgery: Is There a Role for the Antioxidant Melatonin?. Journal of Surgical Research. 152:338–347.

Leick, E.A., Reis, F.G., Honorio-Neves, F.A., Almeida-Reis, R., Prado, C.M., Martins, M.A. and Tiberio, I.F.L.C. 2012. Effects of Repeated Stress on Distal Airway Inflammation, Remodeling and Mechanics in an Animal Model of Chronic Airway Inflammation. Neuroimmunomodulation 19:1–9.

Li, T., Harada, M., Tamada, K. and Nomoto, K., 1997. Repeated restraint stress impairs the antitumor T cell response through its suppressive effect on Th1-type CD4+ T cells. Anticancer Research. 17(6D): 4259-68.

Liu, J. and Mori, A. 1994. Involvement of reactive oxygen species in emotional stress: A hypotesis based on the immobilisation stress-induced oxidative damage and antioxidant defense changes in rat brain, and the effect of antioxidant treatment with reduced glutathione. International Journal of Stress Management 1(3):249-263.

Liu, J., Wang, X. and Mori, A. 1994. Immobilization stress-induced antioxidant defense changes in rat plasma: effect of treatment with reduced glutathione. International Journal of Biochemistry. 26:511–517.

Liu, J.K., Wang, X., Shigenaga, M.K., Yeo, H.C., Mori, A. and Ames, B.N. 1996. Immobilization stress causes oxidative damage to lipid, protein, and DNA in the brain of rats. Official publication of the Federation of American Societies for experimental biology Journal 10 (13): 1532-1538.

Liu, L.Y., Coe, C.L., Swenson, C.A., Kelly, E.A., Kita, H. and Busse, W.W. 2002. School examinations enhance airway inflammation to antigen challenge. American Journal of Respiratory and Critical Care Medicine. 165: 1062–1067.

Maetroni, G.J.M. 2001. The immunotherapeutic potential of melatonin. Expert Opinion on Investigational Drugs 10:467−476.

Marić, D., Kostić, T. and Kovacević, R. 1996. Effects of acute and chronic immobilization stress on rat Leydig cell steroidogenesis. Journal of Steroid Biochemistry and Molecular Biology. 58 (3): 351-5.

McEwen, B.S. 2000. The neurobiology of stress: from serendipity to clinical relevance. Brain Research 886: 172–189.

Meerson, F.Z. 1984. Adaptation, Stress and Prophylaxis. Springer-Verlag Berlin.

Miller, M.M. and McEwen, B.S. 2006. Establishing an agenda for translational research on PTSD. Annals of the New York Academy of Sciences. 1071:294-312.

Moss, G.S. 1972. Pulmonary involvement in hypovolemic shock. Annual Review of Medicine 23: 201-227.

Moss, G.S., Das Gupta, T.K., Newson, B. and Nyhus, L.M. 1972. Morphologic changes in the primate lung after hemorragic shock. Surgery Gynecology and Obstetrics. 134:3-9.

Nagi, H. 2012. Biological studies on the effect of stress on the digestive system of the adultmale albino rat and the possible curative role of diazepam. M. Sc.Thesis, Helwan University, Helwan, Egypt.

Okutan, H., Savas, C. and Delibas, N. 2004. The antioxidant effect of melatonin in lung injury after aortic occlusion–reperfusion. Interactive Cardiovascular and Thoracic Surgery. 3: 519-522.

Othman, A.I., El-Missiry, M.A., Amer, M.A. 2001. The protective action of melatonin on indomethacin-induced gastric and testicular oxidative stress in rats. Journal of Redox Report 6:173–177.

Packer, L. 1985. Mitochondria, oxygen radicals and animal exercise In Membranes and Muscle. International Symposium, Cape Town, March 18-21, IRL Press, Oxford, p 135.

Portela, C.D.P., Tiberio, I.F.L.C., Leick-Maldonado, E.A., Martins, M.A. and Palermo-Neto, J. 2002. Effects of diazepam and stress on lung inflammatory response in OVA-sensitized

rats. American Journal of Physiology. Lung Cellular and Molecular Physiology. 282:L1289–L1295.

Porter, A.G. and Jänicke, R.U. 1999. "Emerging roles of caspase-3 in apoptosis". Cell Death Differentiation. 6 (2): 99–104.

Poyarov, V., Mmyailenko, T., Seredenko, M., Štefanov, A., Kasyanova, E., Lishko, V. and Meerson, F. 1990. Lung stress syndrome and its correction with phospholipids. CR Russ Acad Sci 310 (3): 753-757.

Rai, J., Pandey, S.N. and Srivastava, R.K. 2003. Effect of immobilization stress on spermatogenesis of albino rats. Journal of Anatomical Society of India, 52(1): 55-57.

Rathff, N.B., Wilson, J.W., Hackei, D.B. and Marhn, A.M.Jr. 1970. The lung in hemorrhagic shock II Observations on alveolar and vascular ultrastructure. American Journal of Pathology. 58:353—373.

Reiter, R.J., Tan, D.X., Manchester, L.C., Pilar Terron, M., Flores, L.J. and Koppisepi, S. 2007. "Medical implications of melatonin: receptor-mediated and receptor-independent actions," Advances in Medical Sciences 52: 11–28.

Ritz, T., Steptoe A., DeWilde, S. and Costa, M. 2000. Emotions and stress increase respiratory resistance in asthma. Psychosomatic Medicine 62: 401–412.

Ritz, T. and Kullowatz, A. 2005. Effects of Emotion and Stress on Lung Function in Health and Asthma. Current Respiratory Medicine Reviews 1(2): 209-218.

Şahin, E. and Gümüşlü, S. 2007. Immobilization stress in rat tissues: Alterations in protein oxidation, lipid peroxidation and antioxidant defense system. Comparative Biochemistry and Physiology Part C 144:342–347.

Sakr, S.A., El-Abd, S.F. 2009. Selenium-indused oxidative stress, histological and histochemical alteration in testis of albino rat. Journal of Applied Science. 2(3): 307-317.

Salvesen, G.S. 2002. "Caspases: opening the boxes and interpreting the arrows". Cell Death and Differentiation. 9 (1): 3–5.

Sánchez-Hidalgo, M., Guerrero, J.M., Carrascosa-Salmoral, M.P., Naranjo, M.C., Lardone, P.J. and Alarcón, C. 2009. Decreased MT1 and MT2 melatonin receptor expression in extrapineal tissues of the rat during physiological aging. Journal of Pineal Research. 46: 29–35.

Sapolsky, R.M., Romero, L.M. and Munck, A.U. 2000. How do glucocorticoids influence stress responses? Integrating permissive, suppressive, stimulatory, and preparative actions. Endocrine Reviews 21: 55–89.

Seckin, S., Alptekin, N., Dogru-Abbasoglu, S., Kocak-Toker, N., Toker, G. and Uysal, M. 1997. The effect of chronic stress on hepatic and gastric lipid peroxidation in long-term depletion of glutathione in rats. Pharmacological Research. 36:55–57.

Serel T.A., Özgunner F. and Soyupek S., 2004. Prevention of shock wave-induced renal oxidative stress by melatonin: an experimental study. Urological Research. 32: 69-71.

Tkaczyk, J. and Vizek, M. 2007. Oxidative Stress in the Lung Tissue – Sources of Reactive Oxygen Species and Antioxidant Defence. Prague Medical Report 108 (2):105–114.

Tomas-Zapico, C. and Coto-Montes, A. 2005. A proposed mechanism to explain the stimulatory effect of melatonin on antioxidative enzymes. Journal of Pineal Research. 39: 99–104.

Wohaieb, S.A. and Godin, D.V. 1987. Starvation-related alterations in free radical tissue defense mechanisms in rat. Diabetes 36: 169-173.

Wright, R.J., Rodriguez, M. and Cohen, S. 1998. Review of psychosocial stress and asthma: an integrated biopsychosocial approach. Thorax 53: 1066–1074.

Wright, R.J., Cohen, R.T. and Cohen, S. 2005. The impact of stress on the development and expression of atopy. Current Opinion in Allergy and Clinical Immunology 5: 23–29.

آثارالإجهاد الناجم عن الشلل المستحدث فى ذكور الجرذان البيضاء البالغة على الرئة والدور الوقائي المحتمل للميلاتونين: دراسة بالميكروسكوب الضوئي والالكتروني وهستوكيميائيه مناعيه

هبه كمال محمد

قسم التشريح الادمى والأجنة, كليه الطب, جامعة أسيوط

ملخص البحث

المقدمة: من المعروف أن الإجهاد يعتبر واحدا من أهم الأسباب للعديد من الأمراض كما أن الشلل هو نوع من أنواع الإجهاد الأكثر شيوعا على الحيوانات والإجهاد الناجم عن الشلل قد يساعد على تكوين أنواع الأكسجين التفاعلية، ويمكن أن يؤدي إلى تثبيط جهازالمناعة ويلعب الميلاتونين كمضاد للأكسدة دورا هاما في وظيفة المناعة ومن المعروف أن الرئة لديها سطح كبيرعلى اتصال دائم مع الأكسجين الموجود فى الهواء والملوثات. وهى واحدة من الأعضاء التى تتعرض عادة للإصابة من قبل أنواع الأكسجين التفاعلية والتى تؤدى الى الضرر التأكسدي وتعتبرالرئة مصدررئيسى لإنتاج أنواع الاكسجين التفاعلية.

الهدف من البحث: تهدف الدراسة إلى التحقق من آثار الإجهاد الناجم عن الشلل المستحدث في ذكور الجرذان البالغة على الرئة والدور الوقائي المحتمل للميلاتونين.

المادة و طرق البحث: تم استخدام (45) من ذكور الفئران البالغة تزن (200-250 جم) وتم تقسيم الفئران عشوائيا إلى ثلاث مجموعات متساوية (15فأر لكل منهما). المجموعة (الأولى): ظلت الفئران سليمة وبمثابة المجموعة الضابطة غير المجهدة والمجموعة (الثانية): الفئران التى تعرضت للإجهاد بوضعها على لوحة خشبية مع جذوعها ملفوفة لمدة 90 دقيقة يوميا لمدة 5 أيام فى الأسبوع لمدة 6 أسابيع وكان الحيوان قادرا على تحريك أطرافه ورأسه ولكن غير قادر على تحريك جذعه وفى المجموعة (الثالثة): تعرضت الفئران للإجهاد كما هو موضح سابقا وبالتزامن تم حقن الميلاتونين إلى داخل الغشاء البريتونى بجرعة 10 ملجم / كجم / يوم في تمام الساعة 4:00 مساء وتمت التضحية بجميع الحيوانات فى نفس الوقت عن طريق قطع الرأس تحت تأثير المخدر وتم تشريح الرئتين بها وقسمت العينات من كل مجموعة عشوائيا إلى ثلاث مجموعات فرعية: تمت معالجة المجموعة الأولى للدراسة المجهرية الضوئية بصبغات الهيماتوكسلين والأيوسين والمجموعة الثانية للدراسة بالمجهرالإلكترونى والمجموعة الثالثة للدراسة الهستوكيميائية المناعية بصبغات (كاسباس 3 و iNOS) وقدأجريت دراسات مورفولوجية وإحصائية.

النتائج: أظهر الفحص المجهري الضوئى والإلكترونى الرئتين فى الفئران فى المجموعة الثانية ضررالسنخية الشديد في شكل إنهيارالأكياس والحويصلات الهوائية وزيادة سمك الحاجز بين الأسناخ بشكل ملحوظ لدرجة التعدي على الحويصلات الهوائية والتهابات خلوية ثقيلة وتحلب. وقد أظهرت الخلايا الرئوية من النوع (1) تسنن فى الغشاء النووي ووجود كتل لونين داخل النواة وإنتفاخ الميتوكوندريا وكشفت المجموعة التي تلقت العلاج بالميلاتونين الحد الواضح لجميع التغيرات السنخية وبنية طبيعية تقريبا من القنوات السنخية والكيسات السنخية و الحويصلات الهوائية وأظهرت الدراسة الهستوكيميائية المناعية بصبغات كاسباس 3 و iNOS فى المجموعة الثانية أن التفاعلات المناعية كانت بنية مكثفة وكشفت المجموعة التي تلقت العلاج بالميلاتونين أن التفاعلات المناعية اظهرت انخفاضاً ملحوظاً.

الخلاصة: إن الإجهاد الناجم عن الشلل المستحدث له تأثير ضار على التركيب النسيجي في الرئة وإستخدام الميلاتونين كمادة مضادة للاكسدة قد يكون مفيدا في الوقاية من أثاره الضارة على الرئة.